RSC Advances

PAPER

View Article Online
View Journal | View Issue

Cite this: *RSC Adv.*, 2025, **15**, 8189

Comparison of the effects of perfluoroalkyl and alkyl groups on cellular uptake in short peptides†

Koji Kadota,[a] Ai Kohata, ‡[a] Shinsuke Sando, [bc] Jumpei Morimoto, *[b] Kohsuke Aikawa §*[a] and Takashi Okazoe[ad]

Received 13th January 2025
Accepted 8th March 2025

DOI: 10.1039/d5ra00304k

rsc.li/rsc-advances

The differences in the effects of perfluoroalkyl (R_F) and alkyl (R_H) groups on the cellular uptake of short peptides were evaluated. A facile synthetic method was established to produce Fmoc-protected amino acids bearing R_F and R_H groups on their side chains. The synthesized Fmoc-protected amino acids were successfully incorporated into peptides using solid-phase peptide synthesis. Peptides with an R_F group exhibited higher cellular uptake efficiency compared to peptides with an R_H group of the same side-chain length. Intriguingly, the cytotoxicity of the AF_{647}-R_F-tripeptide ($R_F = C_8F_{17}$) was lower than that of the AF_{647}-R_H-tripeptide ($R_H = C_{12}H_{25}$), despite similar cellular uptake efficiencies. An evaluation of the binding affinity of the peptides to liposome membranes suggested that the higher lipophobicity of the R_F group, compared to the R_H group, contributed to the lower cytotoxicity observed in the peptide with the R_F group. These findings indicate that the introduction of an R_F group into peptides has considerable potential for developing drug-delivery carriers with enhanced uptake efficiency and low cytotoxicity.

Introduction

The perfluoroalkyl (R_F) group is a unique functional group, as R_F-containing compounds exhibit both high hydrophobicity and lipophobicity. R_F-containing compounds exhibit higher hydrophobicity than their hydrocarbon counterparts with the same carbon chain lengths.[1–3] Furthermore, under bulk conditions, perfluoroalkyl compounds form a fluorous phase that is immiscible with both organic and aqueous phases.[4,5] While the differences between R_F and alkyl (R_H) groups, such as oil repellency and phase separation, are commonly observed under bulk conditions, the differences under biologically-relevant low-concentration conditions are not sufficiently understood. One notable biological application of R_F groups is their incorporation into dendrimers[6,7] and polymers.[8,9] Perfluoroalkylation of delivery carriers has been shown to enhance delivery efficiency and biostability while reducing cytotoxicity.[10,11] For example, Cheng and coworkers reported that perfluoroalkylation of branched-polyethyleneimine improves biostability and delivery efficiency.[12] In addition, they reported that fluorinated dendrimers exhibit enhanced cellular uptake efficiency and reduce the nitrogen-phosphorous (N/P) ratio compared to their non-fluorinated dendrimers.[7] Although these studies have compared perfluoroalkylated carriers with their alkylated counterparts, making a precise comparison of the effects of R_F and R_H groups has been challenging because strict control of the introduction efficiency of R_F and R_H groups into these carriers is difficult.

Peptide-based drug-delivery carriers are useful for precisely evaluating the effect of functional groups because peptides can be synthesized in a sequence-defined manner, allowing strict control over the number and position of functional groups within the sequence. A few studies have evaluated peptides containing R_F and R_H groups. Cheng and coworkers investigated the cellular uptake efficiency of peptides containing R_F and R_H groups.[13] Similarly, we have previously evaluated short hydrophobic peptides composed of amino acids bearing R_F and R_H groups.[14,15] Although R_F groups were shown to enhance the cellular uptake of peptides more effectively than R_H groups, the differences between R_F and R_H groups were not systematically investigated, as the primary focus of these studies was on improving cellular uptake efficiency.

In this study, we first evaluated the differences in cellular uptake as well as cytotoxicity between R_F- and R_H-containing short peptides. To understand the underlying reasons for these differences observed in cellular assays, we also compared the

[a]*Department of Chemistry and Biotechnology, Graduate School of Engineering, The University of Tokyo, 2-11-16 Yayoi, Bunkyo-ku, Tokyo, 113-0032, Japan*

[b]*Department of Chemistry and Biotechnology, Graduate School of Engineering, The University of Tokyo, 7-3-1 Hongo, Bunkyo-ku, Tokyo, 113-8656, Japan. E-mail: jmorimoto@chembio.t.u-tokyo.ac.jp*

[c]*Department of Bioengineering, Graduate School of Engineering, The University of Tokyo, 7-3-1 Hongo, Bunkyo-ku, Tokyo, 113-8656, Japan*

[d]*Yokohama Technical Center, AGC Inc., 1-1 Suehiro-cho, Tsurumi-ku, Yokohama 230-0045, Japan*

† Electronic supplementary information (ESI) available. See DOI: https://doi.org/10.1039/d5ra00304k

‡ Current address: School of Life Science and Technology, Institute of Science Tokyo, 4259 Nagatsuta-cho, Yokohama-shi, Kanagawa, 226-8501, Japan.

§ Current address: School of Medicine, Nihon University, 30-1 Oyaguchi-Kamicho, Itabashi-ku, Tokyo, 173-8610, Japan, E-mail: aikawa.kousuke@nihon-u.ac.jp

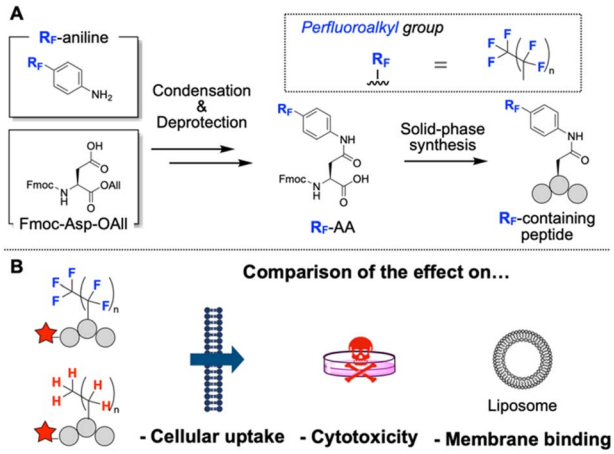

Fig. 1 Schematic illustration of this study. (A) Facile synthetic method of R_F-containing amino acids (R_F-AA) and R_F-containing peptides. (B) Investigation of the differences between R_F- and R_H-containing peptides on cellular uptake, cytotoxicity, and membrane affinity.

membrane affinity of tripeptides containing the R_F and R_H groups. To facilitate the evaluation, we established a facile synthetic method for amino acids and peptides bearing R_F groups (Fig. 1A). Our results demonstrated that the R_F-containing tripeptides exhibit higher cellular uptake efficiency and lower cytotoxicity than their R_H-containing counterparts (Fig. 1B). The R_F-containing tripeptide exhibited lower membrane affinity, possibly accounting for the lower cytotoxicity. These findings provide valuable insights into the development of efficient drug-delivery carriers containing R_F groups.

Result and discussion

Synthesis of amino acids and peptides bearing a perfluoroalkyl (R_F) group

For comparison of the effect of R_F and R_H groups, Fmoc-protected amino acids bearing R_F and R_H groups compatible with solid-phase peptide synthesis (SPPS) are useful, as they allow facile synthesis of peptides with these functional groups at desired positions. We previously synthesized R_F group-containing amino acids (R_F-AAs), which have an R_F group on the α-carbon of glycine.[14] However, the R_F-AAs require multi-step synthesis, have uncontrollable stereochemistry, and exhibit instability under basic conditions because highly acidic α-proton is readily eliminated. Thus, the R_F-AAs could not be utilized in the Fmoc-based SPPS. To overcome these limitations, we aimed to develop novel R_F-AAs that could be easily synthesized and applied to the Fmoc-based SPPS. The synthetic procedure for amino acids bearing R_F groups of various lengths is described in Scheme 1. The synthesis began with the preparation of R_F-nitrobenzene (**1**) *via* a Cu-mediated coupling reaction between 1-iodo-4-nitrobenzene and perfluoroalkyl iodide (R_F–I) according to a conventional procedure.[16] The obtained R_F-nitrobenzene was reduced using Fe/HCl to yield R_F-aniline (**2**). The resultant R_F-aniline was coupled with Fmoc-protected L-aspartic acid allyl ester (Fmoc-Asp-OAll) to afford Fmoc-Asp(R_F)-OAll (**3**). The deprotection of the allyl ester using $Pd_2(dba)_3$/$PhSiH_3$ provided the desired Fmoc-Asp(R_F)-OH (R_F-AAs) (**4**). The same scheme was adopted to synthesize derivatives bearing R_H groups (Scheme S1†). Next, a tripeptide containing R_F-AA or R_H-AA was synthesized using the standard Fmoc-based SPPS. The peptide sequence was identical to that used in our previous study:[14] Ala-X-Phe, where "X" represents the position of the R_F-AA or R_H-AA. This approach enabled the facile synthesis of R_F-AAs in a stereocontrolled manner. Besides, peptides containing R_F-AAs can be synthesized without significant side reactions, such as epimerization.

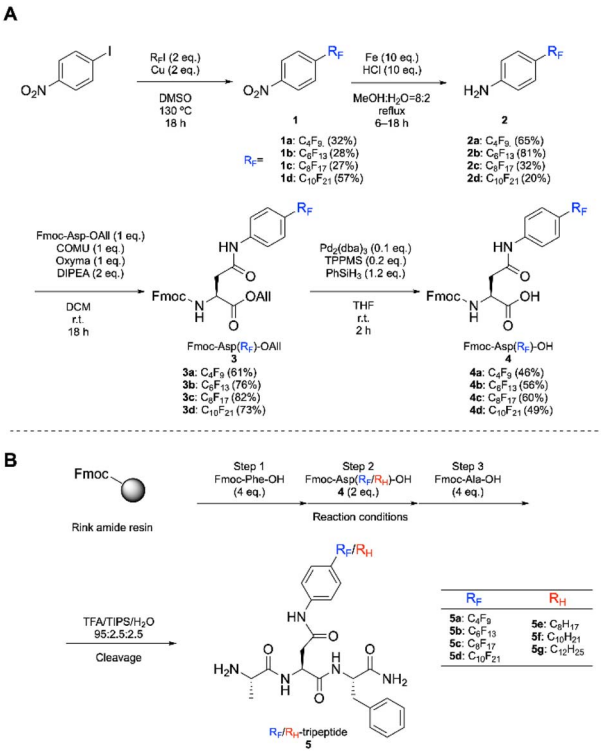

Scheme 1 (A) Synthesis of R_F-containing amino acids (R_F-AAs) and (B) peptides (R_F/R_H-tripeptides). Reaction conditions for the peptide synthesis: Fmoc-AAs-OH (4 eq.), COMU (4 eq.), oxyma (4 eq.), and DIPEA (8 eq.) for 1 h at r.t., then Fmoc group was deprotected by 20% piperidine/DMF for 5 min at r.t., OAll: allyl ester, DMSO: dimethyl sulfoxide, DCM: dichloromethane, MeOH: methanol, THF: tetrahydrofuran, DMF: dimethylformamide, TPPMS: sodium diphenylphosphino-benzene-3-sulfonate, TIPS: triisopropylsilane, TFA: trifluoroacetic acid, COMU: (1-cyano-2-ethoxy-2-oxoethylidenaminooxy)dimethylamino-morpholino-carbenium hexafluorophosphate, oxyma: ethyl 2-cyano-2-(hydroxyimino)acetate, DIPEA: *N*,*N*-diisopropylethylamine.

Given our previous findings that the introduction of a C_8F_{17} enhances the cellular uptake efficiency of peptides,[14] we prepared the tripeptide with $R_F = C_8F_{17}$. To investigate the effect of chain length, we also synthesized tripeptides with R_F groups of varying lengths, including $R_F = C_4F_9$, C_6F_{13}, and $C_{10}F_{21}$. For comparison with the alkylated counterparts, we synthesized a tripeptide with $R_H = C_8H_{17}$, which has the same chain length as $R_F = C_8F_{17}$. Additionally, since the hydrophobicity of a CF_2 unit is reported to be approximately 1.5 times higher than that

of a CH_2 unit,[3] we synthesized a tripeptide containing R_H = $C_{12}H_{25}$ to achieve comparable hydrophobicity to the tripeptide with $R_F = C_8F_{17}$. To further explore the effect of chain length, we also prepared a tripeptide containing R_H = $C_{10}H_{21}$, which represents an intermediate chain length between C_8H_{17} and $C_{12}H_{25}$.

Evaluation of the cellular uptake efficiency of the peptides

The cellular uptake efficiencies of the synthesized peptides were initially investigated using flow cytometry. To visualize cellular uptake, a highly hydrophilic fluorophore, Alexa Fluor 647 (AF_{647}), which is inherently not taken up by cells, was conjugated to the N-terminal amine of the peptides (referred to as AF_{647}-R_F/R_H-tripeptides). AF_{647}-labeled diethylamine (AF_{647}-NEt_2) was employed as a negative control (Fig. 2A). HeLa cells were treated with a serum-free culture medium containing 150 nM of the peptide for 1 h. Serum-free conditions were used to eliminate the potential influence of peptide binding to biomolecules. After washing the cells, cellular uptake efficiency was evaluated by measuring and comparing the fluorescence intensities of the cells using a flow cytometer (Fig. 2B and S1†). Cells treated with peptides bearing an R_F group showed stronger fluorescence intensities than those treated with the corresponding R_H-containing peptides with the same side chain length. For the R_H group, peptides bearing shorter side chains (<C_8H_{17}) showed negligible cellular uptake (data not shown). In contrast, for the R_F group, even the cells treated with the peptides having a short R_F group (C_4F_9) showed a fluorescence signal higher than the cells treated with AF_{647}-NEt_2 control. These results suggest that the introduction of R_F groups into peptides is more effective than the corresponding R_H group in achieving high cellular uptake efficiency.

To investigate the effect of amino acid residues other than R_F or R_H groups on cellular uptake, tripeptides with the general structure Z-Asp(C_8F_{17})-Z were synthesized, where Z represents Phe, Leu, or Pro (Fig. S2 and S3†). The fluorescence intensities of cells treated with the peptides mostly correlated with the hydrophobicity of the peptide sequences, indicating that the hydrophobicity of the peptide plays a critical role in cellular uptake. Based on these results, subsequent evaluations focused primarily on peptides containing C_8F_{17} and $C_{12}H_{25}$ because they exhibited comparable cellular uptake efficiencies.

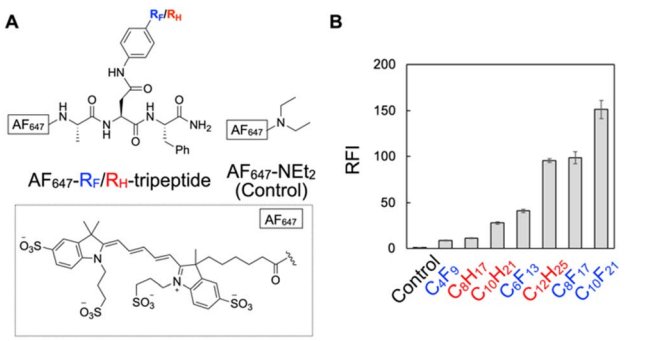

Fig. 2 Evaluation of the cellular uptake efficiency of AF_{647}-R_F/R_H-tripeptides by flow cytometry. (A) Structures of AF_{647}-R_F/R_H-tripeptide and the control (AF_{647}-diethylamine: AF_{647}-NEt_2). (B) Fluorescence intensities of HeLa cells treated with 150 nM of the peptides for 1 h at 37 °C in 5% CO_2 using serum-free medium. Relative fluorescence intensity (RFI) was measured by flow cytometry, with the control serving as a reference.

Investigation of the cellular internalization mechanism

The mechanism of peptide internalization into cells was investigated using endocytosis inhibitors. First, we examined whether the AF_{647}-R_F-tripeptide (R_F = C_8F_{17}) was internalized *via* an energy-dependent pathway, such as endocytosis, or through direct penetration across the cell membrane. When the

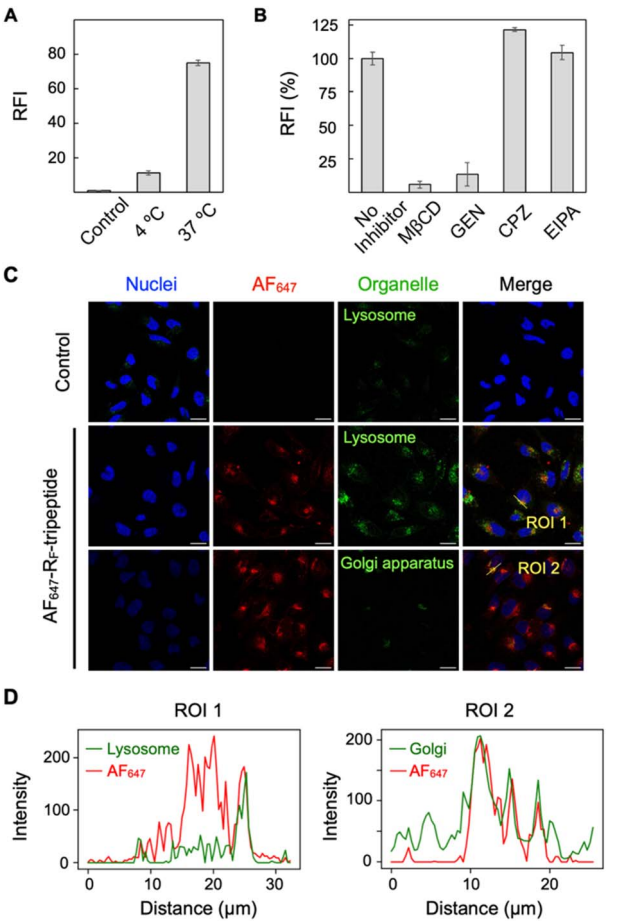

Fig. 3 Investigation of the cellular uptake mechanism and localization of AF_{647}-R_F-tripeptide ($R_F = C_8F_{17}$). (A) Cellular uptake efficiency at 37 °C and 4 °C. (B) Cellular uptake efficiency in the presence of endocytosis inhibitors: 1 mM methyl-β-cyclodextrin (MβCD), 10 μM 5-(*N*-ethyl-*N*-isopropyl)-amiloride (EIPA), 700 μM genistein (GEN), and 10 μM chlorpromazine (CPZ). The error bars represent the standard deviations of triplicates. (C) CLSM images of HeLa cells treated with 150 nM AF_{647}-R_F-tripeptide ($R_F = C_8F_{17}$) and control (AF_{647}-NEt_2) for 1 h at 37 °C, 5% CO_2. Nucleus was stained by Hoechst 33 342 (blue: λ_{ex} = 405 nm and λ_{em} = 420–460 nm), Alexa Fluor 647 fluorescence of AF_{647}-R_F-tripeptide (red: λ_{ex} = 638 nm and λ_{em} = 650–700 nm), and green fluorescence image of LysoTracker green® or Golgi-GFP (green: λ_{ex} = 488 nm and λ_{em} = 500–550 nm). The scale bar indicates 25 μm. (D) Fluorescent intensity profile of region of interest (ROI) analysis. Green line: green fluorescence from organelles (ROI 1: lysosome; ROI 2: Golgi apparatus; red line: AF_{647} fluorescence from the peptide).

cellular uptake experiment was conducted at 4 °C, the fluorescence intensity of the internalized peptide was significantly reduced, indicating that the internalization process is energy-dependent (Fig. 3A). Next, the specific endocytotic pathways involved in the peptide internalization were investigated using four inhibitors of endocytotic pathways: methyl β-cyclodextrin (MβCD, a lipid raft-mediated endocytosis inhibitor); genistein (GEN, a caveolin-dependent endocytosis inhibitor); 5-(*N*-ethyl-*N*-isopropyl)-amiloride (EIPA, a macropinocytosis inhibitor); and chlorpromazine (CPZ, a chlathrin-dependent endocytosis inhibitor). HeLa cells were preincubated with each inhibitor for 30 min prior to the addition of AF_{647}-R_F-tripeptide ($R_F = C_8F_{17}$). EIPA and CPZ did not inhibit the cellular uptake. In contrast, MβCD and GEN largely inhibited cellular uptake (Fig. 3B). A similar result was observed for AF_{647}-R_H-tripeptide ($R_H = C_{12}F_{25}$) (Fig. S4 and S5†). These results indicate that the internalization of AF_{647}-R_F-tripeptide ($R_F = C_8F_{17}$), as well as AF_{647}-R_H-tripeptide ($R_H = C_{12}F_{25}$), occurs primarily *via* lipid raft-mediated and caveolin-dependent endocytosis.

To further understand the internalization process, HeLa cells treated with the peptide were observed using confocal laser scanning microscopy (CLSM). After 1 h of incubation without washing, the peptide was found to be absorbed into the cell membrane (Fig. S6†). To investigate intracellular localization after cellular internalization, cells were incubated with the peptide in the presence of organelle-specific markers. LysoTracker was used to assess whether the peptide underwent a lysosomal pathway, while Golgi-GFP was used to evaluate the potential transport of the tripeptide to the Golgi apparatus, as previous studies have reported that compounds internalized *via* caveolin- and lipid raft-mediated endocytosis are directed to the Golgi apparatus.[17–19] Following 1 h of incubation, residual peptides on the membrane and in the medium were washed away, and the cells were observed under CLSM. Fluorescence signals from the AF_{647}-R_F-tripeptide partially colocalized with both LysoTracker and Golgi-GFP signals (Fig. 3C and D). These results suggest that AF_{647}-R_F-tripeptide ($R_F = C_8F_{17}$) is initially absorbed into the cell membrane, internalizes into cells *via* endocytosis, and is at least partially transported to the Golgi apparatus. The alkyl counterpart ($R_H = C_{12}H_{25}$) exhibited a similar localization pattern to the R_F-containing peptide (Fig. S7†). These results are consistent with previous reports on the behavior of lipophilic molecules, which are internalized *via* caveolin- and lipid raft-mediated endocytosis and subsequently transported to the Golgi apparatus.[17–19]

Investigation of the cytotoxicity differences between peptides containing R_H and R_F groups

Compounds that are efficiently taken up by cells often exhibit cytotoxicity due to their interactions with the cell membrane, which can result in membrane disruption. Therefore, we evaluated the cytotoxicity of the peptides containing R_F and R_H groups (Fig. 4). The cytotoxicity of the peptides against HeLa cells following 1 h of incubation was evaluated using cell-counting kit-8 (CCK-8). The chain length-dependent cytotoxic effect was observed for the AF_{647}-R_F-tripeptide ($R_F = C_6F_{13}$, C_8F_{17}, and $C_{10}F_{21}$) (IC_{50} = 77 ± 7 μM, 41 ± 9 μM, 34 ± 2 μM, respectively) (Fig. S8†). Intriguingly, the cytotoxicity of the AF_{647}-R_F-tripeptide ($R_F = C_8F_{17}$) (IC_{50} = 41 ± 9 μM) was lower than that of the AF_{647}-R_H-tripeptide ($R_H = C_{12}H_{25}$) (IC_{50} = 11 ± 3 μM), despite both peptides achieving similar cellular uptake efficiencies. The result indicates that R_F-containing peptides are useful for achieving efficient cellular uptake with lower cytotoxicity than R_H-containing peptides, consistent with findings reported in previous studies.[7,13,20]

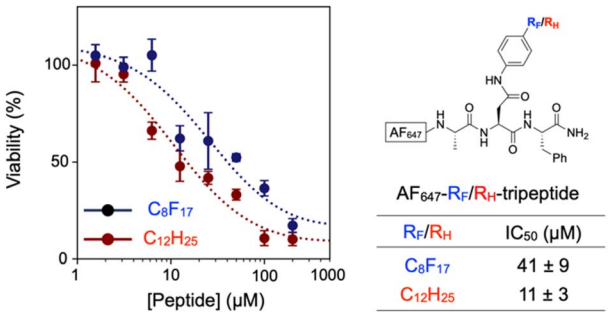

Fig. 4 Cytotoxicity of AF_{647}-R_F/R_H-tripeptides. Cytotoxicity assay using cell-counting kit-8 (CCK-8); 5×10^3 of HeLa cells were treated with the AF_{647}-R_F/R_H-tripeptides for 1 h.

Evaluation of the interaction of peptide with lipid membrane

To elucidate the potential reasons for the differences in cellular uptake efficiency and cytotoxicity between peptides containing R_F and R_H groups, we investigated the interaction of the AF_{647}-R_F-tripeptide ($R_F = C_8F_{17}$) with a model lipid membrane. Giant unilamellar vesicles (GUVs) composed of 1,2-dioleoyl-*sn*-glycero-3-phosphocholine (DOPC) were prepared according to the previously described method.[21] The AF_{647}-R_F-tripeptide (150 nM; $R_F = C_8F_{17}$) was added to the liposome suspension, and its interaction with the membrane was observed under CLSM (Fig. 5A, top). Red fluorescence corresponding to the tripeptide was observed on the surface of the liposomal membrane, indicating that the peptide absorbs into the membrane. This result aligns with earlier CLSM studies on cells, where the peptide was initially observed to adsorb onto the cell membrane. Similar behavior of adsorption on the liposome was also observed for the AF_{647}-R_H-tripeptide ($R_H = C_{12}H_{25}$) (Fig. S9†). In contrast, no fluorescence was observed when the control AF_{647}-NEt_2 was added to the liposome suspension (Fig. 5A, bottom). These results indicate that the peptides interact with membrane lipids through the hydrophobic peptide moieties rather than electrostatic interaction between the anionic fluorescent group and the lipid bilayer.

To compare the relative affinities of the AF_{647}-R_F-tripeptide and AF_{647}-R_H-tripeptide to the liposomal membrane, we measured the zeta potential of the liposomes following the peptide treatment (Fig. 5B, S10, and Table S1†).[22] An increase in the chain length of R_F and R_H groups corresponded to a more negative zeta potential. This observation demonstrated that the peptides with longer R_F and R_H groups are more strongly absorbed into the liposomal membrane. This result suggests

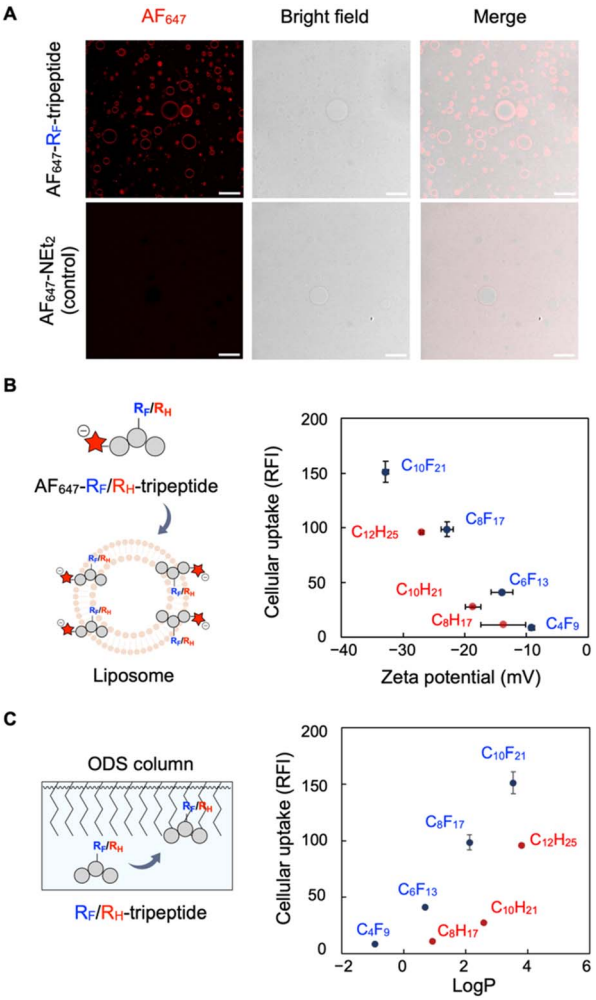

Fig. 5 Membrane affinity of AF_{647}-R_F/R_H-tripeptides. (A) CLSM image of the interaction of AF_{647}-R_F-tripeptide (R_F = C_8F_{17}) and control against DOPC liposome membrane. 150 nM peptide (100 μL) was added to 100 μL of liposome solution (1 mg mL^{-1} lipid). The control (AF_{647}-NEt_2) was used at 750 nM. The scale bar indicates 25 μm. (B) Schematic illustration of membrane affinity of AF_{647}-R_F/R_H-tripeptide (left). Plot of cellular uptake efficiency *versus* zeta-potential of liposome absorbed by AF_{647}-R_F/R_H-tripeptides (right). (C) Schematic illustration of hydrophobicity measurements using ODS column (left). Plot of cellular uptake efficiency *versus* hydrophobicity (Log *P*) of R_F/R_H-tripeptides (right).

that the higher cellular uptake efficiency of peptides with longer R_F/R_H groups is attributable to the higher affinity of the peptides to the cell membrane. Interestingly, AF_{647}-R_H-tripeptide (R_H = $C_{12}H_{25}$) exhibited stronger binding to the liposome than AF_{647}-R_F-tripeptide (R_F = C_8F_{17}), despite both peptides exhibiting similar cellular uptake efficiencies.

The weaker interaction of peptides bearing R_F groups with lipids, as compared to those with R_H group, was further suggested by their retention times on an octadecylsilyl (ODS) column. The retention times of the tripeptides without the N-terminal AF_{647} were measured using a high-performance liquid chromatography (HPLC) system, and the water–octanol partition coefficients (Log *P*) were calculated from the obtained values (Fig. 5C, S11, S12, Tables S2 and S3†). The C_8F_{17}-containing tripeptide exhibited a lower Log *P* value than the $C_{12}H_{25}$-containing tripeptide despite the two peptides having similar cellular uptake efficiencies. Similarly, the C_6F_{13}-containing tripeptide exhibited a lower Log *P* value than the $C_{10}H_{21}$-containing tripeptide, and the C_4F_9-containing tripeptide exhibited a lower Log *P* value than the C_8H_{17}-containing tripeptide, although these two pairs exhibited similar cellular uptake efficiencies. The lower Log *P* values of R_F-containing tripeptides relative to R_H-containing tripeptides with similar cellular uptake efficiencies suggest a weaker interaction of the R_F groups with the alkyl chain of the ODS column due to the lipophobicity of the R_F group.

These combined results suggest that when tripeptides with R_F and R_H groups exhibiting similar cellular uptake efficiencies are compared, tripeptides with R_F groups exhibit lower lipophilicity or higher lipophobicity. The lower lipophilicity of the R_F group may lead to a shorter retention time on the cell membrane, thereby reducing the extent of cell membrane disruption caused by the hydrophobic groups. This could explain the lower cytotoxicity observed for the AF_{647}-R_F-tripeptide compared to the AF_{647}-R_H-tripeptide.

Conclusions

In this study, we aimed to achieve a systematic comparison of the effects of R_F and R_H groups on the cellular uptake efficiency of peptides. The development of a facile synthetic method for Fmoc-protected amino acids bearing R_F and R_H groups with various chain lengths enabled a detailed comparison of their properties.

The comparison of R_F-containing tripeptides and R_H-containing tripeptides showed that the R_F-containing tripeptides exhibit higher cellular uptake efficiency than their R_H-containing counterparts with the same chain length. Intriguingly, when an R_F-containing tripeptide and an R_H-containing tripeptide with similar cellular uptake efficiencies are compared, the R_F-containing tripeptide exhibited lower cytotoxicity. While previous studies have also reported that R_F groups can exhibit lower cytotoxicity than the corresponding R_H groups,[12,23] the underlying reasons for the difference have remained unclear. In this study, liposome binding experiments suggested that when peptides with R_F and R_H groups of similar cellular uptake efficiencies are compared, the R_F-containing peptides exhibit lower lipophilicity, which may account for the lower cytotoxicity.

The effect of R_F modification depends on the peptide sequence and how the peptide is modified by the R_F group. For example, our previous study showed that the stereochemistry of the R_F group in the peptide influences the size of the nanoparticles formed by the peptides, which in turn has a large influence on cellular uptake efficiency. Furthermore, the R_F-modified peptides with high cellular uptake efficiency were found to form nanoparticles with diameters of approximately 100 nm, which were internalized *via* caveolae-dependent endocytosis and micropinocytosis.[14] On the other hand, DLS measurement showed that the C_8F_{17}-modified peptide in this study formed nanoparticles with larger diameters (180 ± 20 nm)

(Fig. S13†) than our previously reported peptide, and the peptide was internalized into the cells *via* lipid raft-mediated and caveolae-dependent endocytosis. Further investigation on the effect of R_F modifications on peptide cellular uptake is required to more comprehensively understand the effect of the R_F modification. The facile synthetic method for R_F-modified peptides established in this study would facilitate the study.

Similar to peptides, oligonucleotides are sequence-defined oligomers that can be systematically modified. A few studies have compared the effects of R_F- and R_H-group modifications on the cellular uptake and cytotoxicity of nucleotides.[24,25] These studies on sequence-defined oligomers, including peptides and oligonucleotides, provide valuable insights into the differences between R_F- and R_H-group modifications.

Although some per- and poly-fluoroalkylated compounds are under regulation because they lead to biological accumulation and environmental pollution,[26] the R_F group has considerable potential in the development of efficient drug-delivery carriers. Appropriate utilization of the R_F group would also be useful in various biological applications such as ^{19}F MRI[27] and Raman imaging.[28]

Data availability

The data used and analyzed during the development of this work is available in the ESI† files accompanying this document.

Author contributions

K. K. conducted the experiments, analyzed the data, and wrote the original draft of the manuscript. K. A. directed the project. A. K., J. M., and S. S. provided advice and discussed the data. T. O. provided advice and the original concept. All the authors contributed to the review and editing of the manuscript.

Conflicts of interest

The authors declare no conflict of interest.

Acknowledgements

We thank Prof. T. Aida at the University of Tokyo for the use of DLS and CLSM instruments. This work was supported by a JSPS KAKENHI Grant-in-Aid for Scientific Research (C) (20K05460) to K. A. and AGC Inc.

Notes and references

1 V. M. Sadtler, F. Giulieri, M. P. Krafft and J. G. Riess, *Chem.–A Eur. J.*, 1998, **4**, 1952–1956.
2 E. Moriyama, J. Lee, Y. Moroi, Y. Abe and T. Takahashi, *Langmuir*, 2005, **21**, 13–18.
3 M. C. Z. Kasuya, S. Nakano, R. Katayama, K. Hatanaka and J. Fluor, *Chem*, 2011, **132**, 202–206.
4 R. Pollice and P. Chen, *J. Am. Chem. Soc.*, 2019, **141**, 3489–3506.
5 M. Cametti, B. Crousse, P. Metrangolo, R. Milani and G. Resnati, *Chem. Soc. Rev.*, 2012, **41**, 31–42.
6 M. Wang and Y. Cheng, *Acta Biomater.*, 2016, **46**, 204–210.
7 M. Wang, H. Liu, L. Li and Y. Cheng, *Nat. Commun.*, 2014, **5**, 1–8.
8 G. Yan, J. Wang, P. Zhang, L. Hu, X. Wang, G. Yang, S. Fu, X. Cheng and R. Tang, *Polym. Chem.*, 2017, **8**, 2063–2073.
9 G. Li, Q. Lei, F. Wang, D. Deng, S. Wang, L. Tian, W. Shen, Y. Cheng, Z. Liu and S. Wu, *Small*, 2019, **15**, 1900936.
10 C. Ge, J. Yang, S. Duan, Y. Liu, F. Meng and L. Yin, *Nano Lett.*, 2020, **20**, 1738–1746.
11 A. Stefanek, K. Łęczycka-Wilk, S. Czarnocka-Śniadała, W. Frąckowiak, J. Graffstein, A. Ryżko, A. Nowak and T. Ciach, *Colloids Surf., B*, 2021, **200**, 111603.
12 Z. Zhang, W. Shen, J. Ling, Y. Yan, J. Hu and Y. Cheng, *Nat. Commun.*, 2018, **9**, 1377.
13 G. Rong, C. Wang, L. Chen, Y. Yan and Y. Cheng, *Sci. Adv.*, 2020, **6**, eaaz1774.
14 K. Kadota, T. Mikami, A. Kohata, J. Morimoto, S. Sando, K. Aikawa and T. Okazoe, *ChemBioChem*, 2023, **24**, e202300374.
15 T. Ono, K. Aikawa, T. Okazoe, J. Morimoto and S. Sando, *Org. Biomol. Chem.*, 2021, **19**, 9386–9389.
16 V. C. R. Mcloughlin and J. Thrower, *Tetrahedron*, 1969, **25**, 5921–5940.
17 A. Chakraborty and N. R. Jana, *J. Phys. Chem. Lett.*, 2015, **6**, 3688–3697.
18 B. Nichols, *J. Cell Sci.*, 2003, **116**, 4707–4714.
19 P. U. Le and I. R. Nabi, *J. Cell Sci.*, 2003, **116**, 1059–1071.
20 Z. Yuan, X. Guo, M. Wei, Y. Xu, Z. Fang, Y. Feng and W.-E. Yuan, *NPG Asia Mater.*, 2020, **12**, 34.
21 K. Tsumoto, Y. Hayashi, J. Tabata and M. Tomita, *Colloids Surf., A*, 2018, **546**, 74–82.
22 N. J. M. Fitzgerald, A. Wargenau, C. Sorenson, J. Pedersen, N. Tufenkji, P. J. Novak and M. F. Simcik, *Environ. Sci. Technol.*, 2018, **52**, 10433–10440.
23 W. Shen, H. Wang, Y. Ling-hu, J. Lv, H. Chang and Y. Cheng, *J. Mater. Chem. B*, 2016, **4**, 6468–6474.
24 G. Godeau, H. Arnion, C. Brun, C. Staedel and P. Barthélémy, *Med. Chem. Commun.*, 2010, **1**, 76–78.
25 M. Narita, A. Kohata, T. Kageyama, H. Watanabe, K. Aikawa, D. Kawaguchi, K. Morihiro, A. Okamoto and T. Okazoe, *ChemBioChem*, 2024, **25**, e202400436.
26 M. G. Evich, M. J. B. Davis, J. P. McCord, B. Acrey, J. A. Awkerman, D. R. U. Knappe, A. B. Lindstrom, T. F. Speth, C. Tebes-Stevens, M. J. Strynar, Z. Wang, E. J. Weber, W. M. Henderson and J. W. Washington, *Science*, 2022, **375**, eabg9065.
27 I. Tirotta, A. Mastropietro, C. Cordiglieri, L. Gazzera, F. Baggi, G. Baselli, M. Grazia Bruzzone, I. Zucca, G. Cavallo, G. Terraneo, F. Baldelli Bombelli, P. Metrangolo and G. Resnati, *J. Am. Chem. Soc.*, 2014, **136**, 8524–8527.
28 C. Chirizzi, C. Morasso, A. A. Caldarone, M. Tommasini, F. Corsi, L. Chaabane, R. Vanna, F. B. Bombelli and P. Metrangolo, *J. Am. Chem. Soc.*, 2021, **143**, 12253–12260.